11^{th} International Conference on Fracture Mechanics of Concrete and Concrete Structures
FraMCoS-11
J. M. Chandra Kishen, A. Ramaswamy, S. Ray and R. Vidyasagar (Eds)
https://doi.org/10.21012/FC11.092371

EXPERIMENTAL INVESTIGATIONS ON THE FRACTURE CHARACTERISTICS OF ULTRA-HIGH PERFORMANCE CONCRETE USING DIFFERENT ASPECT RATIOS

SNEHA* AND SONALISA RAY†

*Research Scholar (Department of Civil Engineering, Indian Institute of Technology Roorkee)
Roorkee, India
e-mail: sneha@ce.iitr.ac.in

†Associate Professor (Department of Civil Engineering, Indian Institute of Technology Roorkee)
Roorkee, India
e-mail: sonalisa.ray@ce.iitr.ac.in

Key words: Ultra-high performance concrete, fibres, Aspect ratio, Fracture energy, Acoustic emission

Abstract. Ultra-high-performance concrete (UHPC) is an advances and novel cementitious composite with superior structural strength and durability properties. A blend of lower water-binder ratio, pozzolanic materials, fillers, and chemical admixtures results in a denser mix, leading to enhanced mechanical and durability properties. The fibre aspect ratio significantly impacts both the mechanical and damage characteristics of Ultra-high performance fibre reinforced concrete (UHPFRC). This research focuses on investigating the impact of fibre aspect ratio on the mechanical and fracture behavior of UHPFRC. Flexural strength tests were conducted on prism specimens $(500mm \times 100mm \times 100\ mm)$ with two different fibre aspect ratios 37.5 and 65. Fracture properties of UHPFRC composites were evaluated using specimens $(700mm \times 150mm \times 80\ mm)$. the nondestructive acoustic emission (AE) technique was utilized to capture fracture characteristics ahead of the crack tip in the presence of different aspect ratio fibre. The results infer that with an increase in aspect ratio from 37.5 to 65, both flexure and fracture strength are superior. Furthermore, the aspect ratio is significantly influencing the post-cracking phase more than that of pre-cracking.

1 INTRODUCTION

Development in the field of construction materials is very progressive. Out of many construction materials like steel, wood, bricks, and clay, concrete is considered to be a highly versatile material. It has been taken to new heights with the development of normal strength concrete (NSC), high strength concrete (HSC), and UHPFRC due to this versatile nature. In comparison to NSC or HSC, UHPFRC has superior mechanical, rheological, and durability properties [1]. UHPFRC is a novel developed material using very fine materials to reproduce a densified particle packing. fibres have an influential role in preventing the development and spread of cracks by providing a bridging force. This bridging force not only enhances the overall material properties but also increases toughness. In addition, incorporating steel fibre in the UHPFRC mix provides enhanced tensile properties and crack resistance, hence widening its applicability towards various civil engineering infrastructures such as bridge and building components, offshore structures, repair re-

habilitation, hydraulic structures, overlay, etc [2]. Steel fibres are added to increase ductility, and these generally transform the developed cracks into multiple cracks of small width, improving the flexural strength and durability of UHPFRC members after post-cracking. Steel fibres and their aspect ratios have greater influence in shaping the properties of structural materials [3]. In recent years several research articles studied the impact of steel fibre. According to Yan et al. [4], the addition of an appropriate amount of steel fibre can substantially enhance both the brittleness and toughness of UHPFRC. Meng et al. [5]and Wu et al. [6] conducted studies on the impact of steel fibre content on the shrinkage performance of UHPFRC. The results revealed that the appropriate addition of steel fibres effectively mitigates local stress concentration and reduces shrinkage. However, excessive fibre content can increase the area of porous, weak interfaces, leading to a decrease in shrinkage inhibition. The splitting tensile strength of UHPFRC is influenced by the fibre aspect ratio, fibre bond factor, and fibre volume fraction [7] To enhance the mechanical properties of UHPFRC, researchers have explored the approach of increasing the aspect ratio of fibres instead of altering the fibre dosage [8–10]. Various study concluded that the first cracking phase has minimal effect or impact on fibre aspect ratio but play an important role in the post-cracking phase [11–13]. Ngo et al. [14] reported that a higher aspect ratio of steel fibres leads to an enhanced load-carrying capacity. But along with mechanical study, the effect of aspect ratio on fracture properties is not explored in detail. Over the past few years, the utilization of the AE technique has gained significant attention as a non-destructive method for monitoring purposes. This technique has been widely employed to effectively characterize the fracture process of quasi-brittle materials [15, 16]. For the large-scale implication of this material in structure, it is of utmost importance to detect and evaluate the severity of any damage present, as this provides a measure of their structural health [17]. Consequently, it becomes essential to thoroughly investigate the fracture mechanism and damage characteristics of UHPFRC. The focus of this study is to investigate the influence of two different steel fibre aspect ratios. Pre-notched UHPFRC beam specimens with two different aspect ration were used for the testing under center-point loading. To evaluate fracture properties, crack mouth opening control testing was performed. To capture fracture characteristics ahead of the crack tip in the presence of different aspect ratio fibres, the AE technique was used throughout the experimentation. Based on the experimental study, flexural strength and fracture parameters were predicted.

2 EXPERIMENTAL PROGRAM

2.1 Material and Mix Proportion

In order to achieve high strength and improved packing density in the UHPFRC composite, fine-grained reactive admixtures are required to be blended with cement. Current work uses silica fume and ground granulated blast furnace slag (GGBFS) to achieve greater strength. In the UHPFRC mix design, the cement was replaced by 22% GGBFS and 10% silica fume. The OPC 43 grade cement is used in this study. The fine aggregate utilized in this study is river sand, with a fineness modulus of 2.68. A polycarboxylic ether-based superplasticizer was utilized to enhance the workability of UHPFRC. To investigate the effect of the different aspect ratios two types of straight micro steel fibres shown in Table 1 were considered with a constant SF volume of 1.5%. The composition of the mix for UHPFRC is given in Table 2.

2.2 Mix Procedure and Sample Preparation

The dry components, including cement, silica fume, GGBFS, and sand, were initially premixed to ensure a uniform dispersion. Subsequently, water containing the superplasti-

cizer was gradually added to the dry mixture while continuously mixing. Once the mixture achieved the desired fluidity and viscosity, the steel fibres were carefully dispersed and incorporated into the mixture. The ten cubes of size $150mm \times 150mm \times 150mm$ were cast to determine the 7-day and 28-day compressive strength. For the flexural testing, six beams were cast for each aspect ratio using dimensions of $100mm \times 100mm \times 500mm$. Furthermore, to examine the fracture properties, four beams, each with dimensions of $700mm \times 150mm \times 80mm$ were cast for every aspect ratio. The notch of depth of 25 mm and width of 3 mm is constructed using the saw cut method three days before the completion of 28 days of curing. Subsequently, the specimens were placed in a room with a temperature of 20 °C for 2-3 days to facilitate the hardening process.

Table 1: Properties of SF

Fibre Type	**Diameter** $d_f(mm)$	**Length** $l_f(mm)$	**Aspect Ratio**	**Density** (g/cm^3)
Type 1	0.16	6	37.5	7.85
Type 2	0.2	13	65	7.85

3 EXPERIMENTAL SETUP

Cube testing for determining the compressive strength was conducted by the guideline outlined in IS 516 [18]. A controls compression testing machine with a capacity of 5000 kN was used to perform the testing. The compressive strength was monitored for the 7th and 28th days of curing. The flexural strength of concrete was evaluated through a four-point bending test using a Controls compression testing machine and the setup is shown in Figure 1. Beams with dimensions of $100mm \times 100 \times 500mm\times$ were tested using BS EN 12390-5 2019 [19]. To investigate the fracture properties of UHPFRC composite, specimens with dimensions $700mm \times 150mm \times 80mm$ were tested in a 500 kN load frame under center-point loading. The tested specimen for both aspect ratios along with setup is shown in Figure 2. The experiments were performed under the crack mouth opening displacement (CMOD) control manner at a loading rate of 0.003 mm/sec. Meanwhile, the crack mouth opening displacement (CMOD) was monitored using a clip gauge equipped with a measuring range of 12 mm.

Table 2: Mix Compostiton of UHPFRC

Constituents	**Quantity** (Kg/cm^3)
Cement	782
GGBFS	253
Sand	115
SP	17.3
Water binder	212.75

4 CALCULATION OF FRACTURE PARAMETERS

4.1 Flexure testing

The flexural strength of the notched UHPFRC beam is determined following the RILEM TC 162-TDF recommendations [20], utilizing Equation 1. In this equation, f_u and P_u represent the flexural strength and peak load from the load-CMOD curves, respectively. The L, b, d, and a_o refer to the span, width, depth, and notch depth, respectively.

$$f_u = \frac{3P_uL}{2b(d-a_o)^2} \tag{1}$$

The residual strengths are determined using Equation2 as per the guidelines outlined in RILEM TC 162-TDF recommendations.

$$f_{R,i} = \frac{3P_{R,i}L}{2b(d-a_o)^2} \tag{2}$$

where,$f_{R,i}$ is the residual flexural strength; $P_{R,i}$ is the load recorded at $CMOD_i$ ($CMOD_{0.5mm}, CMOD_{1.5mm}$, $CMOD_{2.5mm}$, and $CMOD_{3.5mm}$)

4.2 Fracture Energy

The amount of energy required per unit area to open a crack is referred to as fracture energy (G_F). According to a method created by

Hillerborg [21] and used by RILEM TC 50-FMC [22], fracture energy is calculated as the area under the Load-CMOD curve divided by the notched cross-section's area(A_F), as stated in Equation 3

$$G_f = \int \frac{P(\delta)d\delta}{A_F} \tag{3}$$

.

4.3 Acostic emission

Acoustic Emission (AE) is a phenomenon characterized by the generation of transient elastic waves caused by crack propagation, steel bar corrosion, or other forms of deterioration (AE sources). In this research, an eight-channel data acquisition system by MISTRAS was used. The resonant-type differential piezoelectric AE sensors, called R6IAST, function within the 20 to 100-kHz frequency range was used. The AE signal was recorded during the three-point bending test. The AE acquisition system's threshold value was set to 40 dB.

5 RESULTS AND DISCUSSION

The compressive strength was monitored on the 7 and 28 days of curing. The average 7 days and 28 days compression strength is 83.4 and 119 MPa, respectively. The average flexural strength obtained from the four-point bend test for fibre lengths 6 and 13 mm is 9.87 and 18.32 MPa, respectively. The results of both compression and flexural testing are summarized in Table3. The results showed that the fibre aspect ratio significantly affects the hardening properties of UHPFRC. In the context of the flexural test, the load-CMOD curves of the notched specimens are depicted in Figure 3 and 4. These curves demonstrate a predominantly linear trend up to the peak load, succeeded by a ductile post-peak softening phase until reaching deflection values of 9 mm and 11.5 mm for fibre lengths 6 and 13 mm, respectively. The results showed that the fracture flexural strength for notched specimens under the three-point bend test for 6 and 13 mm fibres is 9 MPa and 13 MPa, respectively. This infers that flexural strength with 13 mm fibre is 44% higher than with 6mm fibre. The residual flexural strength results indicated that the fibre with a length of 13 mm represents the sophisticated residual strength but the fibre with 6 mm demonstrated a very low value.

Table 3: Mechanical Parameters of UHPFRC

Concrete Type	**Compressive strength** (MPa)		**Flexural strength** (MPa)	
	7 days	28 Days	Type 1	Type 2
UHPFRC	83.7	119	9.87	18.33

Table 4: Summary of flexural test

Fibre Type	f_u	$f_{R,0.5}$	$f_{R,1.5}$	$f_{R,2.5}$	$f_{R,3.5}$
Type 1	9	7.4	4.1	2.2	1.3
Type 2	13	11.1	9.5	7.1	5.6

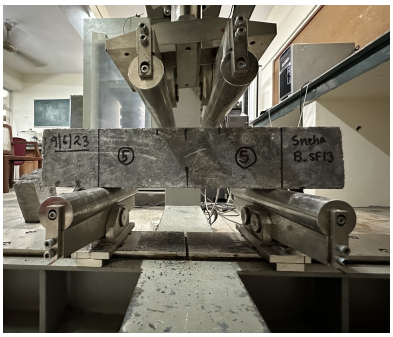

Figure 1: Four-point bend test specimen with 13 fibre length.

Figure 2: Test setup with beam containing 6 and 13 mm fibre.

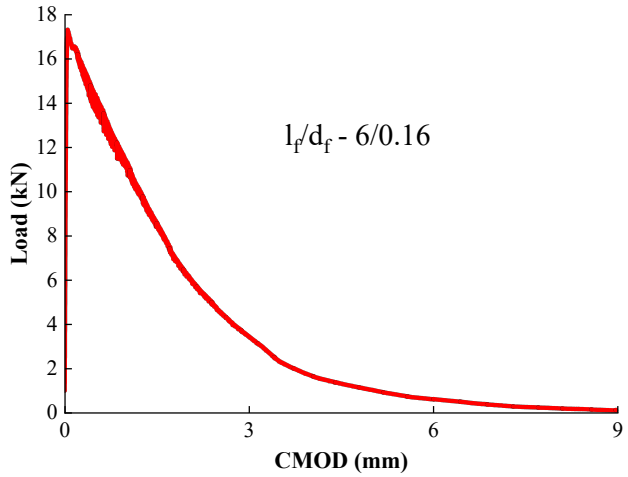

Figure 3: Load-CMOD curve with fibre aspect ratio 37.5.

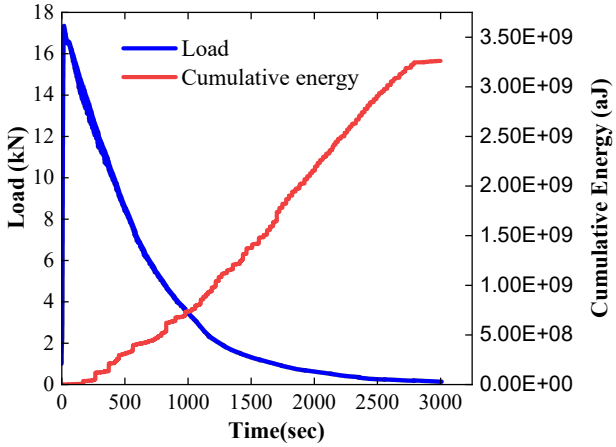

Figure 5: Variation of load and cumulative energy with time for 6 mm fibre length.

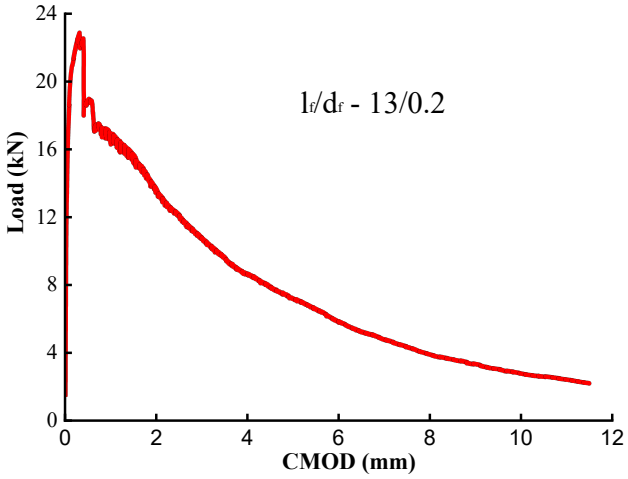

Figure 4: Load-CMOD curve with fibre aspect ratio 65.

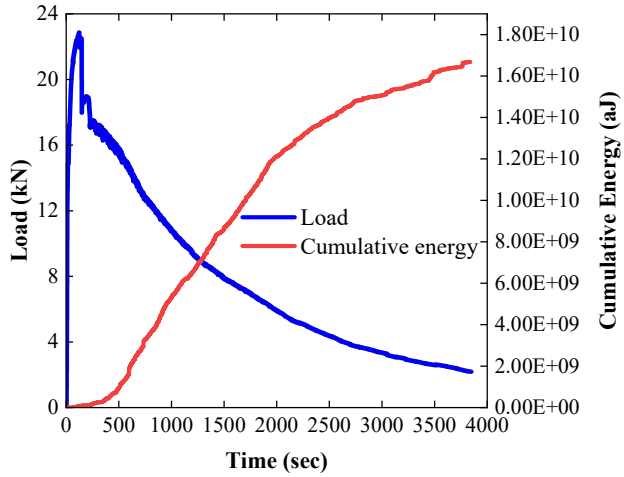

Figure 6: Variation of load and cumulative energy with time for 13 mm fibre length.

The average residual flexural strength results are summarised in Table 4. From the load-CMOD curve, the average fracture energy for two aspect ratio fibres is 2.7 N/mm and 8.95 N/mm respectively. The AE system continuously recorded various AE parameters, including events, absolute energy, time, counts, amplitude, frequency, duration, and others, until the specimens were fractured. The average number of events was found to be 5703 and 8948 for 6 and 13 mm fibre length specimens respectively.

The variation of load and cumulative energy with the time is plotted as shown in Figure 5 and 6 and it shows that with an increase in fibre aspect ratio, there is an increase in the cumulative energy also. In the case of fibre with an aspect of 65, up to the peak load, no absolute energy is recorded. However, beyond approximately 77% of the post-peak load, the cumulative energy demonstrates a more rapid increase, and its keeps on increasing till it reaches its maximum CMOD limit. This shows that the crack is still propagating in a stable state reason being a good bridging mechanism as the distribution is majorly uniform through the cracking

plan. The cumulative energy variation slope is steeper in the case of fibre with an aspect ratio 37.5 because as the crack opening keeps on increasing fibre length is not enough to bridge the cracking. The major reason of the observed behavior could be due to the fact that cracking is mainly governed by the mechanisms of fibre pull-out. During the post-cracking stage, the steel fibres took a major percentage of the tensile load via a load transfer mechanism dependent on the fibre-matrix interfaces. In contrast to the 13 mm fibre length, the bridging is inadequate due to the short fibre length of 6 mm fibre. Similar observations have been reported by researchers i.e., with the constant volume fraction of steel fibre, the flexural strength of UHPFRC exhibits an increment with an increase in the aspect ratio of steel fibre [8]. The steel fibres with larger aspect ratios possessed longer anchorage lengths and stronger bonding interactions with the matrix, resulting in a significant crack propagation deceleration. The study reported that as compared to short fibre larger aspect ratios were more effective in suppressing the formation and expansion of macro cracks, thus improving the flexural strength of UHPFRC [8]. There are previous studies supporting the similar finding as observed in current study that longer steel fibres, possessing higher aspect ratios, exhibit an increased bonding area between the matrix and fibre, resulting in higher strength characteristics. [5, 12, 23].

6 CONCLUSIONS

This research paper investigates the effect of aspect ratio on mechanical properties and fracture parameters of UHPFRC. The findings are summarized as follows

1. Incorporating the constant steel fibre volume of 1.5%, load-carrying capacity under flexural testing with unnotched specimens increases with an increase in fibre aspect ratio from 37.5 to 65.

2. The average flexural strength from a four-point bend for fibre lengths 6 and 13 mm is 9.87 MPa and 18.32 MPa, respectively.

3. Fracture parameters, such as fracture flexural strength, residual flexural strength, and fracture energy, using a notched specimen, demonstrate superior properties when using fibres with a length of 13 mm compared to fibres with a length of 6 mm.

4. The cumulative energy vs. time analysis from the AE study revealed that the aspect ratio of 37.5 exhibited a steep slope, indicating a relatively weaker bridging effect. On the other hand, the aspect ratio of 65 displayed a broader trend, indicating a more pronounced bridging effect.

Acknowledgment

The author would like to thank the Ministry of Education, India for their financial support in the form of the PMRF scholarship.

REFERENCES

[1] ASJ Smith and G Xu. Classification of ultra-high performance concrete (uhpc). *European Journal of Engineering and Technology Research*, 6(6):87–96, 2021.

[2] Darssni Ravichandran, Prabhat Ranjan Prem, Senthil Kumar Kaliyavaradhan, and PS Ambily. Influence of fibers on fresh and hardened properties of ultra high performance concrete (uhpc)—a review. *Journal of Building Engineering*, 57:104922, 2022.

[3] Rajib Kumar Biswas, Farabi Bin Ahmed, Md Ehsanul Haque, Afra Anam Provasha, Zahid Hasan, Faria Hayat, and Debasish Sen. Effects of steel fiber percentage and aspect ratios on fresh and harden properties of ultra-high performance fiber reinforced concrete. *Applied Mechanics*, 2(3):501–515, 2021.

[4] Chang-Wang Yan, Jin-Qing Jia, and Ju Zhang. Experimental study of ra-

tio between splitting tensile strength and compressive strength for steel fiber reinforced ultra high strength concrete. *Journal of Dalian University of Technology*, 52(2):233–238, 2012.

[5] Weina Meng, Yiming Yao, Barzin Mobasher, and Kamal Henri Khayat. Effects of loading rate and notch-to-depth ratio of notched beams on flexural performance of ultra-high-performance concrete. *Cement and Concrete Composites*, 83:349–359, 2017.

[6] LM Wu, Caijun Shi, Zuhua Zhang, and H Wang. Effects of steel fiber on drying shrinkage of ultra high performance concrete. *Materials Review*, 31(12):58–65, 2017.

[7] Hamdy K Shehab El-Din, Heba A Mohamed, Mahmoud Abd El-Hak Khater, and Sayed Ahmed. Effect of steel fibers on behavior of ultra high performance concrete. In *International Interactive Symposium on Ultra-High Performance Concrete*, volume 1. Iowa State University Digital Press, 2016.

[8] Xinyi Yan, Yuxin Gao, Yaoling Luo, Yao Bi, and Yuhao Xie. Effect of different steel fiber types on mechanical properties of ultra-high performance concrete. In *IOP Conference Series: Materials Science and Engineering*, volume 1167, page 012001. IOP Publishing, 2021.

[9] Doo-Yeol Yoo, Su-Tae Kang, and Young-Soo Yoon. Enhancing the flexural performance of ultra-high-performance concrete using long steel fibers. *Composite Structures*, 147:220–230, 2016.

[10] Gum Sung Ryu, Su Tae Kang, Jung Jun Park, Kyung Taek Koh, and Sung Wook Kim. Mechanical behavior of uhpc (ultra high performance concrete) according to hybrid use of steel fibers. *Advanced Materials Research*, 287:453–457, 2011.

[11] Doo-Yeol Yoo, Joo-Ha Lee, and Young-Soo Yoon. Effect of fiber content on mechanical and fracture properties of ultra high performance fiber reinforced cementitious composites. *Composite structures*, 106:742–753, 2013.

[12] Doo-Yeol Yoo, Soonho Kim, Gi-Joon Park, Jung-Jun Park, and Sung-Wook Kim. Effects of fiber shape, aspect ratio, and volume fraction on flexural behavior of ultra-high-performance fiber-reinforced cement composites. *Composite Structures*, 174:375–388, 2017.

[13] Doo-Yeol Yoo, Su-Tea Kang, and Young-Soo Yoon. Effect of fiber length and placement method on flexural behavior, tension-softening curve, and fiber distribution characteristics of uhpfrc. *Construction and Building materials*, 64:67–81, 2014.

[14] Tri Thuong Ngo, Jun Kil Park, and Dong Joo Kim. Loading rate effect on crack velocity in ultra-high-performance fiber-reinforced concrete. *Construction and Building Materials*, 197:548–558, 2019.

[15] Awadhesh Sharma, Sonalisa Ray, and MA Iqbal. Characterization of fracture development in geometrical similar ultra-high-performance concrete (uhpc) beams using acoustic emission (ae) technique. *Materials Today: Proceedings*, 2023.

[16] Dinesh K. Samal and Sonalisa Ray. An improved understanding of the influence of w/c ratio and interfacial transition zone on fracture mechanisms in concrete. *Magazine of Concrete Research*, 75(16):847–863, 2023.

[17] Antoine Boniface, Jacqueline Saliba, Zoubir Mehdi Sbartaï, Narintsoa Ranaivomanana, and Jean-Paul Balayssac. Evaluation of the acoustic emission 3d localisation accuracy for the mechanical dam-

age monitoring in concrete. *Engineering Fracture Mechanics*, 223:106742, 2020.

[18] IS 516: 2014. Method of tests for strength of concrete, 2004.

[19] British Standard. Testing hardened concrete. *Compressive Strength of Test Specimens, BS EN*, pages 12390–3, 2009.

[20] Lucie Vandewalle, D Nemegeer, L Balazs, B Barr, Joaquim Barros, P Bartos, Nemkumar Banthia, M Criswell, E Denarie, M Di Prisco, et al. Rilem tc 162-tdf: Test and design methods for steel fibre reinforced concrete'-sigma-epsilon-design method-final recommendation. *Materials and Structures*, 36(262):560–567, 2003.

[21] Arne Hillerborg. The theoretical basis of a method to determine the fracture energy gf of concrete. *Materials and structures*, 18:291–296, 1985.

[22] RILEM Draft Recommendation. Determination of the fracture energy of mortar and concrete by means of three-point bend tests on notched beames. *Materials and structures*, 18(106):285–290, 1985.

[23] Doo-Yeol Yoo and Nemkumar Banthia. Mechanical properties of ultra-high-performance fiber-reinforced concrete: A review. *Cement and Concrete Composites*, 73:267–280, 2016.